iScience

CellPress

Article

Genetic Landscape of Somatic Mutations in a Large Cohort of Sporadic Medullary Thyroid Carcinomas Studied by Next-Generation Targeted Sequencing

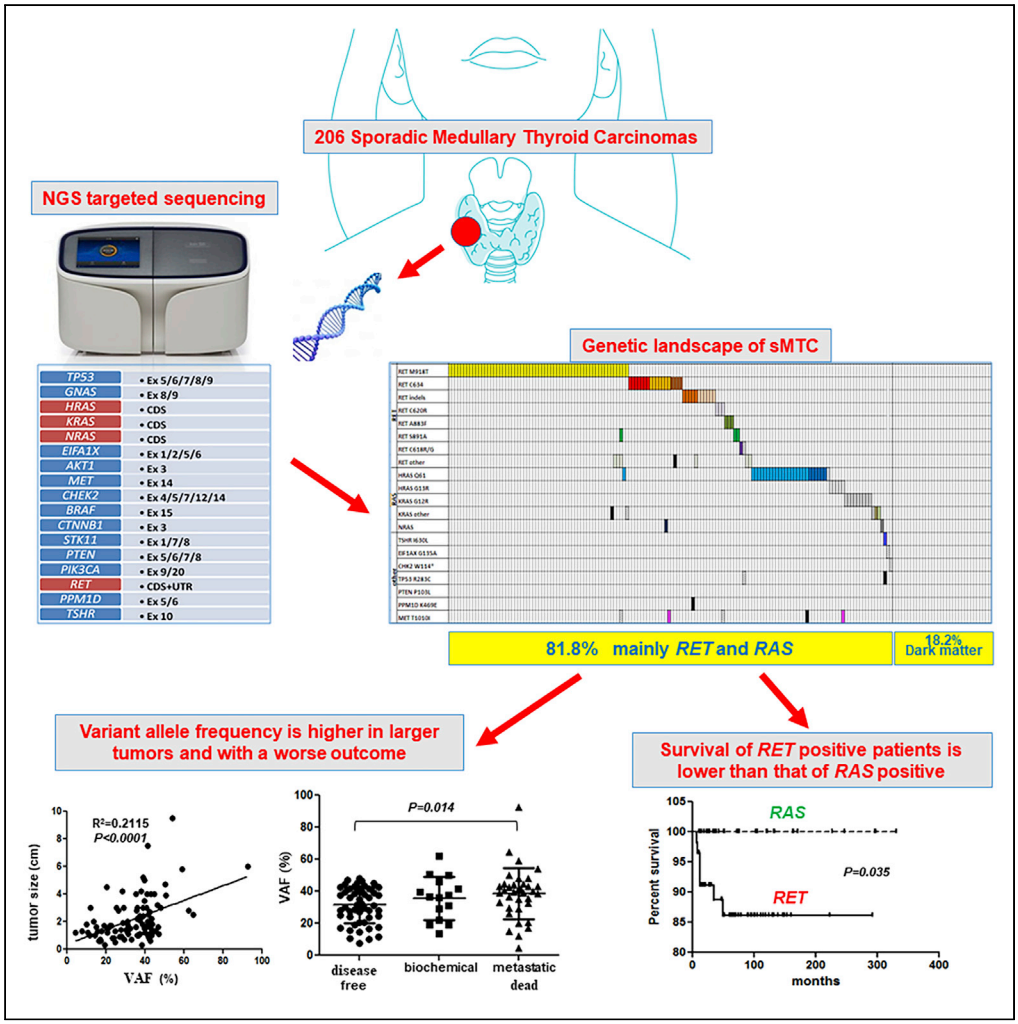

Raffaele Ciampi, Cristina Romei, Teresa Ramone, ..., Clara Ugolini, Fulvio Basolo, Rossella Elisei

raffaele.ciampi@unipi.it

HIGHLIGHTS

We studied by NGS the largest cohort of sporadic MTC that has been studied so far

RET and *RAS* mutations have been confirmed as the major drivers in sporadic MTC

Allele frequency can be considered a new marker of bad prognosis in *RET*-mutated cases

Survival rate is significantly shorter in *RET*-mutated than in *RAS*-mutated cases

Ciampi et al., iScience *20*, 324–336
October 25, 2019
https://doi.org/10.1016/j.isci.2019.09.030

iScience

CellPress

Article

Genetic Landscape of Somatic Mutations in a Large Cohort of Sporadic Medullary Thyroid Carcinomas Studied by Next-Generation Targeted Sequencing

Raffaele Ciampi,[1,3,5,*] Cristina Romei,[1,3] Teresa Ramone,[1] Alessandro Prete,[1] Alessia Tacito,[1] Virginia Cappagli,[1] Valeria Bottici,[1] David Viola,[1] Liborio Torregrossa,[2] Clara Ugolini,[2] Fulvio Basolo,[2] and Rossella Elisei[1,4]

SUMMARY

Sporadic Medullary Thyroid Carcinoma (sMTC) is a rare but aggressive thyroid tumor. *RET* and *RAS* genes are present in about 50%–80% of cases, but most of the remaining cases are still orphan of a genetic driver. We studied the largest series of sMTC by deep sequencing to define the mutational landscape. With this methodology we greatly reduced the number of *RET*- or *RAS*-negative cases and we confirmed the central role of *RET* and *RAS* mutations. Moreover, we highlighted the bad prognostic role of *RET* mutations in sMTC and consolidated the favorable prognostic role of *RAS* mutations. For the first time, we showed that the variant allele frequency represents an additional prognostic marker inside the group of *RET*-mutated sMTC.

INTRODUCTION

Medullary Thyroid Carcinoma (MTC) originates from neural crest-derived parafollicular C-cells and can occur in hereditary (25%) or sporadic forms (75%) (Kouvaraki et al., 2005). Germline-activating *RET* mutations are found in 95%–98% of hereditary MTC, whereas somatic *RET* mutations are present in 25%–40% of sporadic MTC (sMTC) (Cerrato et al., 2009; Drosten and Putzer, 2006; Kouvaraki et al., 2005; Romei et al., 2011). Several types of somatic *RET* mutations have been reported in sMTC, with the most common mutation occurring in codon M918 within exon 16, which is present in up to 90% of *RET*-positive cases, followed by mutations in codon C634 within exon 11 (Elisei et al., 2014; Eng et al., 1994; Romei et al., 2016).

The presence of *RET* somatic mutations in sMTC has been shown to have a negative prognostic value (Elisei et al., 2008). In addition to point mutations, aneuploidy of chromosome 10 and *RET* gene amplification have been described in MTC cases, prevalently in cases with a somatic *RET* mutation (Ciampi et al., 2012).

Recently, activating point mutations in *RAS* genes (*H-*, *K-*, and *NRAS*) has been described in *RET*-negative sMTC, with a variable percentage depending on the different series and screening techniques employed (Agrawal et al., 2013; Boichard et al., 2012; Ciampi et al., 2013; Moura et al., 2015, 2011). *RAS* gene point mutations in MTC mainly occur in *H-* and *KRAS*, and they are usually mutually exclusive with *RET* mutations. In our previous study, we found that patients harboring *RAS* mutations showed a better prognosis than those harboring *RET* mutations or presenting no mutations (Ciampi et al., 2013).

Despite the presence of *RET* and *RAS* somatic mutations, 20–50% sMTC are still orphans of a genetic driver. Assessing the mutational status, especially for the *RET* gene, is crucial for targeted therapies with tyrosine kinase inhibitors currently employed, such as vandetanib and cabozantinib (Elisei et al., 2013; Wells et al., 2010), and the discovery of new oncogene alterations remains crucial to individuate novel targets for this type of therapy.

The recent advent of next-generation sequencing (NGS) techniques has dramatically changed our understanding of cancer genomics with the discovery of novel genetic alterations responsible for the pathogenesis of several cancer types (Berger and Mardis, 2018).

In these recent years, NGS has been applied in endocrine research as well (Persani et al., 2018), and several reports have been published for MTC, in some cases using a whole-exome approach (Agrawal et al., 2013; Chang et al., 2018) but mainly targeted sequencing (Heilmann et al., 2016; Ji et al., 2015; Simbolo et al.,

[1]Unit of Endocrinology, Department of Clinical and Experimental Medicine, University-Hospital of Pisa, Pisa 56124 Italy

[2]Department of Surgical, Medical, Molecular Pathology and Critical Area, University-Hospital of Pisa, Pisa 56124 Italy

[3]These authors contributed equally

[4]Senior author

[5]Lead Contact

*Correspondence: raffaele.ciampi@unipi.it

https://doi.org/10.1016/j.isci.2019.09.030

2014; Wei et al., 2016). According to the results reported in these studies, despite the presence of some rare events present in a few cases, the common occurrence of mutually exclusive *RET* and *RAS* mutations has been confirmed to be the main pathogenic signature of sMTC. The few novel alterations found in these studies represent more likely a "private" mutation of that specific tumor than significantly recurrent genetic alterations. The major limits of these previous studies are the relative low number of cases analyzed and few data about the correlation between the mutations and clinical and pathological features of the tumors.

We aimed to analyze a large series of sMTC by NGS targeted sequencing using a thyroid-specific gene mutation panel to delineate their mutational landscape and correlate the molecular data with the pathological characteristics of the tumors and with both the clinical features and outcome of patients affected with sMTC.

RESULTS

Sequencing Metrics and Overview of Gene Alterations Detected by NGS Targeted Sequencing

Of 209 cases studied, 28 were excluded as not informative due to technical reasons or insufficient quality of data obtained. Informative sequencing data were then obtained for 181/209 (86.6%) sMTC. The mean value of the variant vertical coverage obtained was 2,038X (median, 2,049.5; range, 117.7–5,713), and the mean number of reads for the sample was 385,564.1 (median, 396,496.5; range, 21,198–1,744,507).

In total, 166 genetic alterations were detected in 148 sMTC cases (Table S1). In particular, we found 152 single-nucleotide variations and 14 indels: 107/166 (64.5%) were found in the *RET* protooncogene, 48/166 (28.9%) in the three *RAS* genes (*HRAS*, *KRAS*, *NRAS*), 5/166 (3%) in the *MET* gene, 2/166 (1.2%) in the *TP53* gene, 1/166 (0.6%) in the *TSH* receptor (TSHR) gene, 1/166 (0.6%) in the *EIF1AX* gene, 1/166 (0.6%) in the *CHK2* gene, and 1/166 (0.6%) in the*PPM1D* gene. One hundred fifty-four gene alterations were validated by Sanger direct sequencing and confirmed to be somatic, five were found to be germline, one was confirmed in tissue DNA, but blood was not available for germline validation, and six were not validated by Sanger direct sequencing due to low Variation Allele Frequency (VAF) values or for other technical reasons.

All the mutations that were previously detected by Sanger sequencing for somatic *RET* and *RAS* mutations were confirmed by NGS while in eight cases we observed a discrepancy with a previous negative result by Sanger and a positive one by NGS. This apparent discrepancy was due either to the low VAF that was under the detection limit of Sanger (<20%) or bad Sanger sequencing quality.

Analysis of Genetic Alterations Occurring in sMTC Cases

General Distribution of Mutations

As shown in Table S1, the number of cases harboring one or more genetic alterations was 148/181 (81.7%), whereas the remaining 33/181 (18.3%) did not carry any alteration targeted in our panel. In particular, 132/148 (89.2%) mutated cases harbored one single mutation, whereas 11/148 (7.4%) showed a heterogeneous pattern due to the presence of a somatic driver mutation coupled with one or more other somatic mutations and 5/148 (3.4%) harbored one somatic driver mutation coupled with a second germline mutation (Table 1).

Types of Mutations

Cases presenting *RET* somatic alterations as the driver were 101/181 (55.8%): in 88 cases as a single alteration and in 13 cases as multiple alterations. Cases presenting *RAS* mutations as the driver were 44/181 (24.3%): in 42 cases as a single mutation and 2 cases in association with either a somatic or germline *MET* T1010I mutation. Finally, 3/181 (1.6%) cases presented mutations in other genes (i.e., *CHK2* W114*, *EIF1AX* G135A, and *TSHR* I630L) (Table S1). The remaining 33/181 (18.3%) were negative for all alterations targeted in our panel.

RET Mutations: Prevalence, Types, and Associations with Other Mutations

As shown in Figure 1, 60/148 (40.5%) mutated sMTC harbored the *RET* M918T mutation. In 54 cases, it was present as a single mutation; and in 6 cases, it was associated with other *RET* (n = 3) or *RAS* mutations (n = 3). The details of associated mutations are reported in Table 1. The *RET* gene C634 codon was mutated

No	Alteration 1	Alteration 2	Alteration 3	Alteration 4
41	*RET* M918T (s) [47.3%]	*RET* D925A (s) [46.7%]		
242	*RET* M918T (s) [32.2%]	*RET* R297H (s) [11.8%]		
196	*RET* M918T (s) [12.3%]	*RET* R833C (s) [25.0%]	*RET* S891A (s) [20.3%]	*MET* T1010I (n.v.) [18.6%]
140	*RET* M918T (s) [39.0%]	*KRAS* K182E (n.v.) [20.0%]		
176	*RET* C634W (s) [17.3%]	*NRAS* A18V (s) [7.5%]		
253	*RET* C634W (s) [11.6%]	*MET* T1010I (s) [50.1%]		
132	*RET* D898_E901del (s) [30.9%]	*RET* S904P (s) [30.8%]		
169	*RET* C620R (s) [41.5%]	*MET* T1010I (n.v.) [6.7%]		
3	*RET* C618G (n.v.) [40.5%]	*TP53* R283C (n.v.) [48.1%]		
251	*HRAS* G13R (s) [23.3%]	*MET* T1010I (s) [8.3%]		
39	*HRAS* Q61R (s) [34.4%]	*RET* M918T (s) [3.0%]		
88	*RET* M918T (s) [19.7%]	***KRAS A130V (g) [44.9%]***		
91	*RET* C634Y (s) [37.3%]	***RET R215L (g) [49.9%]***		
201	*RET* D898_E901del (s) [26.6%]	***PPM1D K469E (g) [37.5%]***		
20	*HRAS* Q61R (s) [41.7%]	***MET T1010I (g) [51.4%]***		
52	*TSHR* I630L (s) [31.0]	***TP53 R158C (g) [52.8%]***		

Table 1. List of Cases Presenting Multiple Somatic Alterations and Somatic Coupled with a Germ-Line Alteration (in bold). Variant Allele Frequency (VAF) Values Are Reported in Brackets

(s), verified somatic; (n.v.), not detectable by direct sequencing.

in 18/148 (12.2%) cases with different aminoacidic alterations (Figure 1). In 15 cases, it was present as a single mutation, whereas, in 3 cases, it was associated with other alterations. A *RET* indel was present in 14/148 (9.5%) cases (Table S1 and Figure 1): in 12 cases, it was present as a single mutation, while in 2 cases it was associated with other alterations. Additionally, 3/148 (2%) cases presented the C620R mutation, and one of them harbored a simultaneous *MET* T1010I mutation. Another 2/148 (1.3%) cases showed a C618R mutation, and one of them had a simultaneous *TP53* R283C mutation. Finally, 2/148 (1.3%) cases presented the *RET* S891A mutation, and 1/148 (0.7%) cases showed the *RET* C630R and 1/148 (0.7%) cases showed the *RET* S1024F mutation. Among cases harboring *RET* multiple mutations, cases n. 41 and 132 presented the *RET* M918T + D925A and *RET* D898_E902del + S904P mutations, respectively. The analysis of the specific sequencing reads associated with these mutations showed that they were very close and on the same allele (i.e., in *–cis*), likely consequent to a single mutational event (data not shown). A complete detailed description of these mutations is summarized in Table S1 and Figure 1.

RAS Mutations: Prevalence, Types, and Associations with Other Mutations

Alterations of the three *RAS* genes were present in 44/148 (29.7%) mutated cases. Of 148 sMTC cases, 31 (20.9%) were mutated in the *HRAS* gene and included 2 cases with a simultaneous somatic or germline *MET* T1010I mutation, respectively (Figure 1). Another 12/148 (8.2%) cases were positive in *KRAS*, and only 1/148 (0.7%) presented the *NRAS* Q61K mutation (Table S1 and Figure 1).

Other Unconventional Mutations: Prevalence, Types, and Associations

Only 3/148 (2%) sMTC cases harbored single mutations in other genes belonging to our panel, such as *CHK2* W114*, *EIF1AX* G135A, and *TSHR* I630L. The last case was also associated with a germline *TP53* R158C mutation. Although the *TSHR* I630L mutation has been validated as somatic, the other two mutations could not be, and consequently, we could not establish their potential driver role.

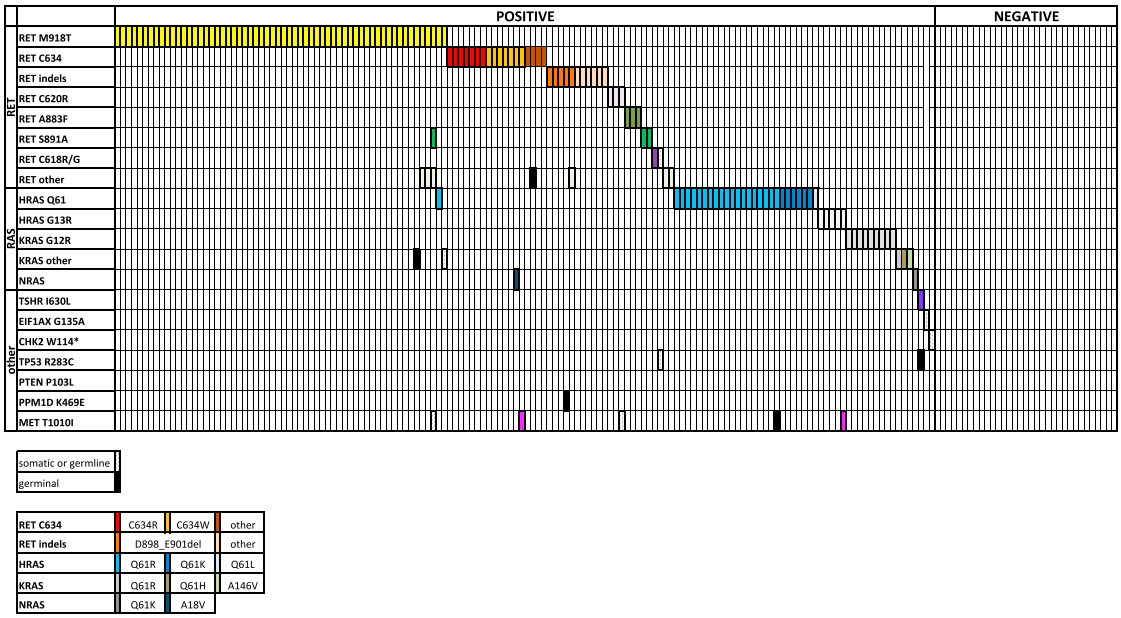

Figure 1. Mutational Landscape of sMTC

Mutational profile of the 168 informative sMTC cases identified by NGS analysis. Each column corresponds to a single case. Genetic variations are listed on the left. The colored squares correspond to somatic mutations, whereas the black squares correspond to germline mutations, all validated by Sanger sequencing. Squares with a point-pattern represent mutations that were not validated by Sanger or not confirmed to be somatic or germline. See also Table S1.

Rare and Uncommon Mutations In the Analyzed Genes

As shown in Table 2, among the above-reported mutations, we found a series of 18 uncommon and/or novel alterations. With the exception of the somatic or germline *MET* T1010I mutation, which was present in five separate cases already harboring either *RET* or *RAS* alterations (Table 3), all the others were single mutations in single cases. Considering their rarity and according to the *in silico* analysis (i.e., Clinic Var and MutTaster prediction tests) and public database of known gene alterations (i.e., dbSNP and COSMIC and HGMD), we hypothesized that they could be private mutations whose driver role in the pathogenesis of the sMTC is unclear (Table 3).

TERT Promoter C228 and C250 Mutational Status

The sequencing data for the *TERT* promoter were available for 148/181 (81.8%) cases. Neither C228T nor C250T mutations were found in any of the studied cases.

Whole-Exome Sequencing

The whole-exome sequencing (WES), despite the wide and deep analysis, did not reveal any other recurrent somatic mutation either in the four sMTC negative at the targeted sequencing or in those already known to be *RET* mutated.

Correlation of the Mutational Status of Primary sMTC with the Clinical and Pathological Features of the Patients

The 175/209 (83.7%) sMTC cases, whose primary tumor was analyzed, were divided into four categories depending on the mutational status (*RET* M918T, *RET* other, *RAS* mutations, and not *RET*/not *RAS*) and were correlated with the clinical and pathological features of the patients (Table 4). A statistically significant correlation was found between the presence of *RET* mutations, both together and when considering M918T alone, and the advanced stage of the disease ($p = 0.0025$), higher T category ($p < 0.0001$), and the presence of both lymph-node (N) ($p = 0.0021$) and distant metastases (M) ($p = 0.0073$).

In contrast to *RET*-mutated cases, *RAS*-mutated sMTC cases were significantly associated with a better outcome ($p = 0.001$), a lower stage of disease ($p = 0.0037$), and lower T category (i.e., T1/T2)

Case	Gene Mutation	VAF (%)	Status	dbSNP ID	MAF	COSMIC ID α HGMD ID β	ClinVar Prediction γ MutTaster Prediction δ	Notes
88	*KRAS* c.389C > T; p.A130V	44.9	Germ line	rs730880473	<0.01	COSM4169153 α	Uncertain significance γ	Simultaneous *RET* M918T (s); reported as "neutral" (Wang et al., 2019)
41	*RET* c.2774A > C; p.D925A	46.7	Somatic	Novel	–	Novel	Disease causing δ	Occurring in *-cis* with *RET* M918T (s)
242	*RET* c.890G > A; p.R297H	11.8	Somatic	Novel	–	Novel	Polymorphism δ	Simultaneous *RET* M918T (s)
196	*RET* c.2497C > T; p.R833C	25	Somatic	rs377767422	<0.01	CM068590 β	Likely pathogenic γ	Simultaneous *RET* M918T (s)
20,169, 196251,253	*MET* c.3029C > T; p.T1010I	Various	Somatic; germ line	rs56391007	<0.01	COSM707 α CM118113 β	Conflicting results δ	
176	*NRAS* c.53C > T; p.A18V	7.5	Somatic	Novel	–	Novel	Disease causing δ	Simultaneous *RET* C634W (s)
91	*RET* c.644G > T; R215L	49.9	Germ line	rs748128929	<0.01	–	Polymorphism δ	Simultaneous *RET* C634Y (s)
201	*PPM1D* c.1405A > G; p.K469E	37.5	Germ line	rs61756416	<0.01	–	Disease causing δ	Simultaneous *RET* E898_E901del (s); reported as "benign" in breast and ovarian cancer (Ruark et al., 2013)
132	*RET* c.2710T > C; p.S904P	30.8	Somatic	Novel	–	Novel	Disease causing δ	Occurring in *-cis* with *RET* E898_E901del (s)
128	*RET* c.1908_1909insTGCCG CACG; p.T636_V637delinsCRT	35.4	Somatic	rs377767437	–	CI983210 β	Likely pathogenic γ	Described germ-line in MEN2A (Höppner et al., 1998)
122	*RET* c.1886_1891delTGTGCG; p.L629_D631delinsH	38.4	Somatic	NA	–	COSM27040 α	–	Likely driver
302	*RET* c.1894_1902delGAGCT GTGC; p.E632_C634del	42.9	Somatic	Novel	–	Novel	–	Likely driver
252	*RET* c.3071C > T; p.S1024F	17.6	Somatic	Novel	–	Novel	Disease causing δ	Likely driver
3	*TP53* c.847C > T; p.R283C	48.1	n.v.	rs149633775	<0.01	COSM10911 α/CM041458 β	Conflicting results δ	Simultaneous *RET* C618G (s)
52	*TSHR* c.1888A > C; p.I630L	31	Somatic	–	–	COSM26432 α/ CM100952 β	Disease causing δ	Simultaneous *TP53* R158C (g)
52	*TP53* c.472C > T; p.R158C	52.8	Germinal	rs587780068	<0.01	COSM43848 α/ CM121763 β	Pathogenic γ	Simultaneous *TSHR* I630L (s)
196	*EIF1AX* c.404G > C; G135A	41.4	n.v.	Novel		Novel	Disease causing δ	
198	*CHK2* c.341G > A; W114*	10.1	n.v. in blood	Novel		Novel	Disease causing δ	

Table 2. Details of Unconventional Alterations Found by NGS Targeted Sequencing

n.v., not detectable by direct sequencing.

N.	Somatic Mutation	MET T1010I
196	*RET* M918T (s) [12.3%] *RET* S891A (s) [20.3%] *RET* R833C (s) [25.0%]	*MET* T1010I (n.v.) [18.6%]
253	*RET* C634W (s) [11.6%]	*MET* T1010I (s) [50.1%]
169	*RET* C620R (s) [41.5%]	*MET* T1010I (n.v.) [6.7%]
110	*HRAS* Q61R (s) [41.7%]	*MET* T1010I (g) [51.4%]
251	*HRAS* G13R (s) [23.2%]	*MET* T1010I (s) [8.3%]

Table 3. List of Cases Presenting the *MET* T1010I Mutation in Association with *RET* or *RAS* Somatic Mutations
Variant allele frequency (VAF) value is reported in brackets.
(s), verified somatic; (g), verified germinal; (n.v.), not detectable by direct sequencing.

($p = 0.0015$), but no correlation was observed between the presence of *RAS* mutation and other epidemiological and pathological features (Table 5).

A strong correlation was also found between the presence of *RET* mutations and a worse patient outcome ($p < 0.0001$), and the survival of Kaplan-Meier curves confirmed that patients with sMTC harboring the *RET* mutation had a higher rate of cancer-related deaths than patients harboring *RAS* mutations (log rank = 4.41; $p = 0.035$) (Figure 2).

Correlation of the Variant Allele Frequency Value with the Tumor Size and Outcome of the Patients

The overall mean VAF of the mutations found was 35.1% (median, 30.2; range, 4.4–95.2). However, a big difference in VAF was observed among different cases with the lowest VAF observed in the rare and uncommon alterations (Table S1). According to the VAF, we could hypothesize the role of the mutations, especially in those cases with more than one alteration: the mutation with the greatest VAF would likely be the driver mutation (Li et al., 2017).

As shown in Figure 3, panel A1, when we compared in 95 patients with primary tumor the VAF value of the driver mutation, any type, with the sMTC tumor size (in centimeters), we observed that larger tumors harbored mutations with a higher VAF value ($p < 0.0001$). However, when we performed the same analysis in subgroups according to the type of mutation, the correlation was confirmed in the subgroups of *RET*-mutated cases, either when all *RET* (Figure 3, panel A2) or only *RET* M918T-mutated cases were considered (Figure 3, panel A3) ($p < 0.0001$ and $p = 0.0013$, respectively) but not in the subgroup harboring *RAS* mutations (Figure 3, panel A4).

Analyzing 103 patients, a higher VAF value of the driver mutation was also correlated with a worse outcome of the patients, as demonstrated by a significantly higher VAF value in patients with metastatic disease with respect to disease-free patients, both when considering all cases with any type of mutation ($p = 0.003$) (Figure 3, panel B1) and when analyzing the subgroup with only *RET* mutations ($p = 0.047$) (Figure 3, panel B2). By contrast, this correlation was not found in the subgroup with only *RAS*-positive cases (Figure 3, panel B3).

DISCUSSION

In recent years, the introduction of NGS techniques has revolutionized research and the diagnosis of many diseases, including endocrine diseases (Persani et al., 2018). In particular, cancer research was hugely improved by this high-throughput techniques, being able to sequence large genome and transcript portions and increasing the probability of discovering novel mutations, especially in less frequently studied genes (Berger and Mardis, 2018; Kamps et al., 2017).

Several studies have been performed in MTC, both employing WES (Agrawal et al., 2013; Chang et al., 2018) and targeted sequencing with specific panels of gene mutations (Heilmann et al., 2016; Ji et al., 2015; Simbolo et al., 2014; Wei et al., 2016). In summary, these studies confirmed the role of *RET* and *RAS* somatic mutations as main drivers in the pathogenesis of sMTC; on the other hand, very few alternative

	RET M918T	*RET* Other	*RAS*	Not *RET*/Not *RAS*	p Value
Sex					0.1378[a]
Female	51.2% (22/43)	52.8% (19/36)	72.5%(29/40)	67.9% (19/28)	
Male	48.8% (21/43)	47.2% (17/36)	27.5% (11/40)	32.1% (9/28)	
Age at diagnosis (mean ± SD) (years)	49.43 ± 13.93	55.67 ± 14.32	55.81 ± 15.44	58.84 ± 15.70	0.0779[b]
Primary/metastases					0.1609[a]
Primary	74.1% (43/58)	83.7% (36/43)	90.9% (40/44)	84.8% (28/33)	
Metastases	25.9% (15/58)	16.3% (7/43)	9.1% (4/44)	15.2% (5/33)	
Outcome					<0.0001[a]
Disease-free	26.3% (10/38)	66.7% (20/30)	61.8% (21/34)	77.3% (17/22)	
Biochemical	7.9% (3/38)	6.7% (2/30)	29.4% (10/34)	9.1% (2/22)	
Metastatic/dead	65.8% (25/38)	26.6% (8/30)	8.8% (3/34)	13.6% (3/22)	
Stage					0.0001 [a]
I	18.9% (7/37)	46.9% (15/32)	62.5% (25/40)	70.8% (17/24)	
III	81.1% (30/37)	53.1% (17/32)	37.5% (15/40)	29.2% (7/24)	
T Categories					<0.0001[a]
T1+T2	37.1% (13/35)	72.7% (24/33)	90.0% (36/40)	83.3% (20/24)	
T3+T4	62.9% (22/35)	27.3% (9/33)	10.0% (4/40)	16.7% (4/24)	
Lymph-node metastasis (N)					0.0021[a]
N0	30.6% (11/36)	54.5% (18/33)	66.7% (26/39)	75.0% (18/24)	
N1	69.4% (25/36)	45.5% (15/33)	33.3% (13/39)	25.0% (6/24)	
Distant metastasis (M)					0.0073[a]
M0	77.8% (28/36)	90.6% (29/32)	97.5% (39/40)	100.0% (24/24)	
M1	22.2% (8/36)	9.4% (3/32)	2.5% (1/40)	0 (0/24)	

Table 4. Correlation between Mutational Status of *RET* and *RAS* Genes with Clinical and Pathological Features of the Primary sMTC Cases

Unless stated, values are expressed in % (number/total number).

[a]Chi-squared test.

[b]One-way ANOVA test.

genetic alterations have been discovered, still leaving a rather large portion of cases negative for common somatic gene alterations.

In the present study, we characterized 181 sMTCs by NGS targeted sequencing, and this series represents, to our knowledge, the largest analyzed so far. For this purpose, we designed a custom gene mutational panel that includes all amplicons covering the entire coding region of the *RET*, *HRAS*, *KRAS*, and *NRAS* genes that are known to be involved in C-cell tumorigenesis (Ciampi et al., 2013) and all the known gene alterations involved in follicular thyroid cancer tumorigenesis (Nikiforov et al., 2014; Nikiforova et al., 2013).

Our data showed that 55.8% of cases harbored *RET* genetic alterations, confirming that *RET*, particularly the M918T mutation, is the main driver oncogene in sMTC. The second main driver oncogene has been confirmed to be *RAS*, particularly *HRAS* and *KRAS* genes, which were altered in 24.3% of sMTC cases. Only a small subgroup, representing only 1.6% of cases, showed other types of uncommon mutations

	RAS+	*RAS-*	p Value
Sex			0.089[a]
Female	72.5% (29/40)	56.4% (62/110)	
Male	27.5% (11/40)	43.6% (48/110)	
Age at diagnosis (mean ± SD)	55.81 ± 15.44	58.84 ± 15.70	0.571[b]
Outcome			0.0003[a]
Disease-free	61.8% (21/34)	52.2% (47/90)	
Biochemical	29.4% (10/34)	7.8% (7/90)	
Metastatic/dead	8.8% (3/34)	40% (36/90)	
Stage			0.0037 [a]
I + II	62.5% (25/40)	41.5% (39/94)	
III + IV	37.5% (15/40)	58.5% (55/94)	
T Categories			0.0015[a]
T1+T2	90.0% (36/40)	62.4% (58/93)	
T3+T4	10.0% (4/40)	37.6% (35/93)	
Lymph-node metastasis (N)			0.0857[a]
N0	66.7% (26/39)	49.5% (46/93)	
N1	33.3% (13/39)	50.5% (47/93)	
Distant metastasis (M)			0.107[a]
M0	97.5% (39/40)	88.2% (82/93)	
M1	2.5% (1/40)	11.8 (11/93)	

Table 5. Association of *RAS*-Mutated sMTC Cases and Clinical and Pathological Features

Unless stated, values are expressed in % (number/total number).

[a]Chi-squared test.

[b]Student Unpaired t test.

whose driver role remains unclear. According to these results, the prevalence of complete negative cases in our series was narrowed to 18.3% of cases (Figure 1), which increased up to 19.9% if we include the subgroup with the uncommon mutations. In agreement with the results of other two studies (Agrawal et al., 2013; Chang et al., 2018), also in our hands the WES was unable to identify other recurrence mutations that could further reduce this subgroup of negative cases. It is conceivable that for these cases other types of genetic and/or epigenetic alterations can play a role.

Compared with previous data obtained analyzing sMTC by Sanger direct sequencing (Ciampi et al., 2013; Elisei et al., 2008), we obtained an overall higher number of mutated cases, especially for *RAS* positive cases and, at the same time, we reduced the negative or "mutational orphan" sMTC cases. These results strongly support the use, whenever possible, of deep-sequencing techniques whose sensitivity is significantly higher than that of Sanger sequencing; this is a very important aspect to address, especially in metastatic patients who could benefit from targeted therapy whose choice largely depends on the knowledge of mutational status (Viola et al., 2016).

In our series, most cases harbored single mutually exclusive alterations (89.2%), whereas only a small portion of cases (7.4%) harbored multiple somatic mutations (Table 1), demonstrating that, genetically, sMTC is a rather stable tumor similar to what has been shown for papillary thyroid carcinoma (Cancer Genome Atlas Research Network, 2014). Moreover, according to the VAF values in the mutations, 9/11 cases harboring multiple somatic mutations showed a higher VAF of the *RET* mutation than that of the additional mutations, thus suggesting the driver role of *RET* also in these heterogeneous cases. It is

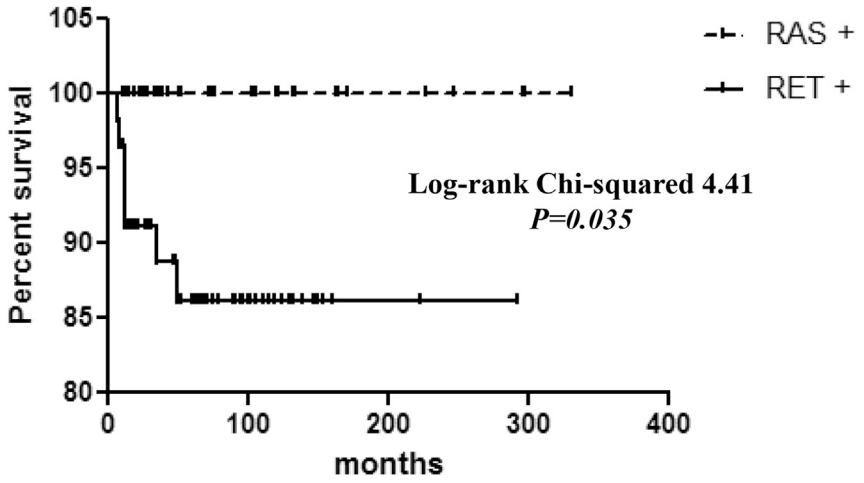

Figure 2. Survival in *RET*- and *RAS*-Mutated sMTC Cases

Kaplan-Meier curves showing survival in patients with sMTC harboring *RET* mutations or *RAS* mutations. The difference in the curves was statistically significant (log rank = 4.41; p = 0.035) and demonstrated that *RET*-positive cases have a higher probability to die of the disease.

noteworthy that, in two of four cases with two simultaneous *RET* mutations (Table 1, cases 41 and 132), the VAF was the same. This finding, combined with the observation that the mutations were closely mapping in –*cis* within the same sequencing read, indicates that they might be the result of a single simultaneous mutational event in a single allele of the same cell and not truly heterogeneous mutations, thus reducing the percentage of "true" heterogeneous cases to 6.5% of sMTC.

In some cases, the VAF observed in additional mutations was rather low and, in several cases, they represented "novel" mutations never described before and with an uncertain pathogenic role (Table 2). The meaning of these mutations is unknown, but being aware of their presence can be relevant for the follow-up of the patients because, if selected, these mutations could be responsible for acquired resistance during therapy with kinase inhibitors (Camidge et al., 2014; Chen and Fu, 2011), and their presence should not be overlooked.

We also found five cases in which a germinal mutation of key genes in thyroid tumorigenesis was also present and whose real pathogenic role is unclear (Table 1). These five alterations have been already reported in the dbSNP database, although VAF <0.01 excludes them as common SNPs (Table 2). The rarity of these alterations in the normal population suggests some pathogenic role for the tumor (Li et al., 2017), although *in silico* predictive scores describe only some of them as pathogenic. In particular, two of them (i.e, *KRAS* A130V and *PPM1D* K469E) have been described as non-pathogenic/neutral alterations (Ruark et al., 2013; Wang et al., 2019). Even less is known about the new somatic indel mutation (i.e., *RET* c.1894_1902delGAGCTGTGC; p.E632_C634del) that has never been described previously (Table 2).

Among cases presenting multiple mutations we did not find any difference in terms of number and type of mutations when comparing cases in which we analyzed the primary tumor tissues with in which we analyzed the metastatic lesions. The most recurrent additional mutation (5/181, 2.8%) observed in our series was the *MET* T1010I point mutation that was present at either the somatic or the germinal level (Table 3), as demonstrated also by the VAF (i.e., approximately 50% when germinal and less than 20% when somatic). In our series, *MET* T1010I was always associated to a driver mutation either in *RET* or *RAS* gene. The T1010I mutation is located in exon 14 of the *MET* gene encoding for the juxtamembrane portion of the tyrosine kinase (Comoglio et al., 2018) and exon 14 alterations, which are described in different tumor types, might be crucial for activation of the *MET* oncogene (Vigna et al., 1999). Germinal and/or somatic *MET* T1010I mutations have been described in several tumor types (Comoglio et al., 2018), including thyroid tumors (Wasenius et al., 2005). In this last study, 104 thyroid tumors were analyzed and somatic or germline *MET* T1010I mutations were found in 7% of samples: particularly, 1/12 (8.3%) sMTC harbored a germline *MET* T1010I. We also found either somatic (4/5) or germline (1/5) *MET*T1010I-mutated cases, but all of them were characterized by the presence of another mutation likely driving the tumoral transformation.

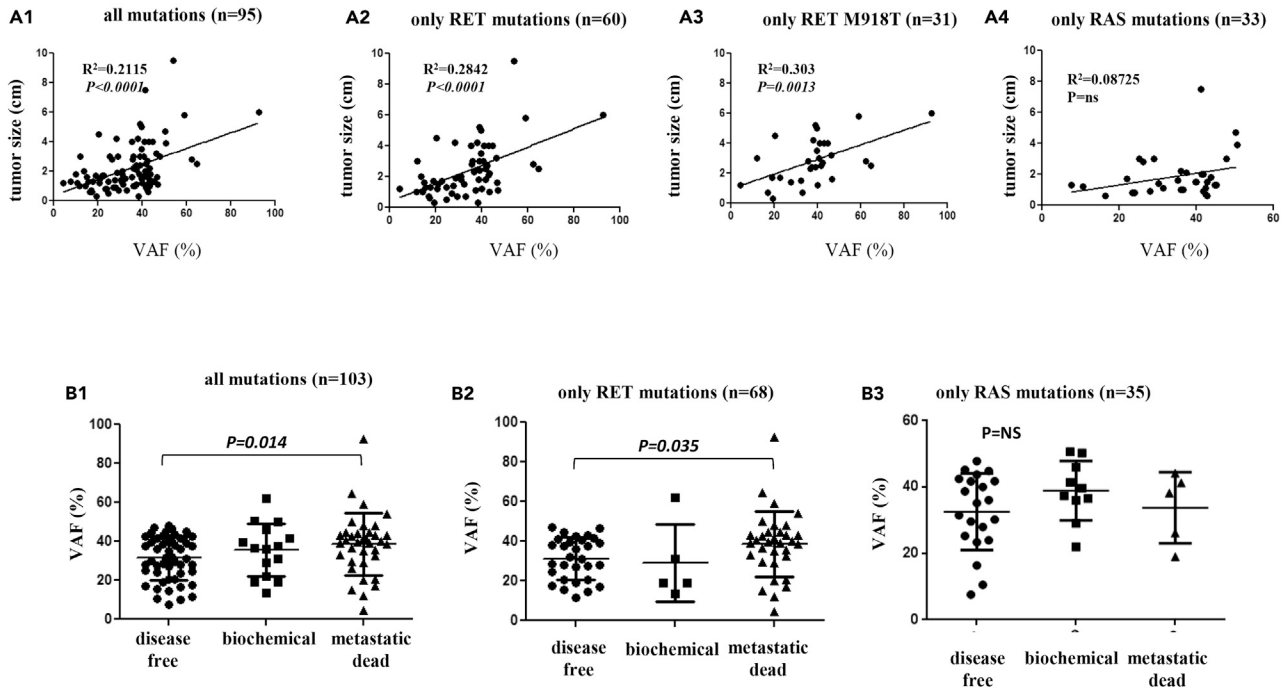

Figure 3. Correlation of the Variant Allele Frequency with Tumor Size and Outcome of Patients with sMTC

(A) Correlation between the tumor size (cm) and VAF of the driver mutation in sMTC. The comparison considered all mutations (A1), only *RET* mutations (A2), only the *RET* M918T mutation (A3), and only *RAS* mutations (A4). In all cases, except *RAS*-mutated cases, a statistically significant difference was observed (A1: $p < 0.0001$; A2: $p < 0.0001$; A3: $p = 0.0013$; A4: p = ns).

(B) Correlation between the VAF value (%) of the driver mutations and outcome of patients when considering all mutations (B1), only *RET* mutations (B2), and only *RAS* mutations (B3). The differences between the outcome categories were significant between disease-free and metastatic patients in the former two cases (B1: $p = 0.003$; B2: $p = 0.0047$; ANOVA), whereas no difference was observed considering only *RAS* mutations (B3: p = ns). Data are represented as mean ± SEM.

In general, the role of this mutation in cancer is not fully understood, and conflicting results exist, especially in other human tumors. As suggested for other human cancers (Neklason et al., 2011), a predisposing role of *MET* T1010I, especially when present at the germline level, might be hypothesized also for sMTC.

Other than describing the oncogene mutations involved in the pathogenesis of sMTC, we also compared the mutational status of these tumors with the clinical and pathological features of patients (Table 4). The presence of *RET* mutations and, in particular, the M918T was confirmed to be significantly associated with a worse outcome, a higher tumoral staging, a higher T category, and the presence of lymph-node and distant metastases. Moreover, when we compared the survival Kaplan-Meier curves of patients with sMTC with *RET* or *RAS* somatic mutations, a significantly lower percentage of surviving patients in the *RET*-positive cases was found. These results confirmed in a much larger series our previously reported data (Ciampi et al., 2013; Elisei et al., 2008) and those recently collected in a meta-analysis summarizing the clinical significance of the mutational status in MTC (Vuong et al., 2018).

Simultaneously, we observed that *RAS*-positive cases were significantly associated with a better outcome, a lower tumor staging, and a lower rate of T categories than *RET*-positive cases, and, also when compared with the *RAS* negative cases, independent from the presence of *RET* mutation (Table 5). With these results, we confirmed that sMTC with *RAS* mutations have, in general, a less aggressive phenotype and a better prognosis as we previously observed (Ciampi et al., 2013) and herein, as definitively demonstrated by the virtually 100% rate of survival of patients harboring *RAS* mutations (Figure 2).

Compared with previous studies, using the NGS approach, we could also evaluate the VAF value, adding a parameter that it is not possible to evaluate using Sanger direct sequencing. The mutated allele abundance has been demonstrated to be a prognostic factor itself in tumors, including PTC, in which a higher

BRAF V600E VAF predicts a poorer outcome (Guerra et al., 2012). Our results demonstrated that, also in this series, larger tumors not only are more frequently *RET* mutated but also have a higher VAF that corresponds to a higher percentage of mutated cells. This observation suggests that the presence of a *RET*-mutated allele, particularly M918T, confers a growth advantage and results in larger clonal tumors. These findings are also in line with our previous observation of a lower rate of *RET* M918T mutation in micro-MTC that, when mutated, likely harbored a much lower VAF of the *RET* mutation not detectable with the traditional Sanger sequencing (Romei et al., 2012). Moreover, we demonstrated that a higher VAF correlated with a poorer prognosis, both when considering all mutations and when considering only *RET* mutations. According to these findings, VAF may be included in the list of bad prognostic markers in the subgroup of *RET*-mutated sMTC cases.

By contrast, *RAS*-mutated tumors appear to be clonal also in smaller tumors and no difference in the outcome of patients was observed compared with the *RAS*-mutated allele abundance. Based on this observation, we can hypothesize that two different sMTC types, in terms of both development and aggressiveness, might exist (i.e., *RET*-like and *RAS*-like) and further studies are needed to confirm this hypothesis.

Finally, we studied most of the sMTC for the presence of mutations in the *TERT* gene promoter hotspots (C228, C250), and, conversely, regarding what happens to other thyroid neoplasms (Alzahrani et al., 2016), *TERT* promoter mutations in C228 and C250, at least in our study, do not play any role in the pathogenesis and/or progression of sMTC.

In conclusion, in the present study, that included the largest series of sMTC studied so far by NGS, we confirmed that *RET* and *RAS* gene alterations are the main actors in driving the development of this rare human tumor. Moreover, we reinforced the concept that *RET*-mutated cases have a more aggressive phenotype and a poorer prognosis, particularly when the VAF is higher, so that this parameter can be considered a new marker of a worse prognosis in *RET*-mutated sMTC. At the same time, we demonstrated that *RAS*-mutated cases have a better outcome than *RET*-mutated cases. Finally, a lower-than-expected percentage of sMTC cases are still orphans of a recognized genetic driver, and further studies for alternative mechanisms of tumor transformation need to be performed.

Limitations of the Study

The main limitation of this study is that we used a custom targeting sequencing panel including a large series of genes involved in thyroid cancer pathogenesis that failed in providing evidence of strong alternative mechanisms of pathogenesis besides *RET* and *RAS* mutations. Although in some cases WES analysis was also performed, the possibility that other alterations may be involved cannot be completely ruled out with this study.

METHODS

All methods can be found in the accompanying Transparent Methods supplemental file.

DATA AND CODE AVAILABILITY

For the following novel mutation a submission to COSMIC DATABASE has been requested and an identifier **COSP47106** has been generated by COSMIC as a proof of successful data submission.

RET c.2774A>C; p.D925A

RET c.890G>A; p.R297H

NRAS c.53C>T; p.A18V

RET c.2710T>C; p.S904P

RET c.1894_1902delGAGCTGTGC; p.E632_C634del

RET c.3071C>T; p.S1024F

EIF1AX c.404G>C; G135A

CHK2 c.341G>A; W114*

SUPPLEMENTAL INFORMATION

Supplemental Information can be found online at https://doi.org/10.1016/j.isci.2019.09.030.

ACKNOWLEDGMENTS

This study has been supported by grants to R.E. from Associazione Italiana per la Ricerca sul Cancro (AIRC, Investigator grant 2018, project code 21790), Agenzia Italiana del Farmaco (AIFA, project code AIFA-2016-02365049), and Progetto di Ricerca di Ateneo (PRA_2018_27) from University of Pisa.

AUTHOR CONTRIBUTIONS

R.C. and C.R. were responsible for the major part of the project, its design, and analysis of data. T.R. provided major technical support in collecting samples and nucleic acid extraction. A.P. provided clinical and pathological data from the patients and statistical assistance. A.T. performed the TERT promoter sequencing. V.C., D.V., and V.B. were responsible for recruiting the patients and collecting blood samples and informed consents. L.T., C.U., and F.B. provided FFPE tumor samples and were the pathologists responsible for all the histology classification of tumors. R.C. and R.E. wrote the manuscript. R.E. is the senior author and responsible for the supervision of the project.

DECLARATION OF INTERESTS

The authors declare that there are no conflicts of interest that could affect the impartiality of the reported research.

Received: May 20, 2019
Revised: August 1, 2019
Accepted: September 23, 2019
Published: October 25, 2019

REFERENCES

Agrawal, N., Jiao, Y., Sausen, M., Leary, R., Bettegowda, C., Roberts, N.J., Bhan, S., Ho, A.S., Khan, Z., Bishop, J., et al. (2013). Exomic sequencing of medullary thyroid cancer reveals dominant and mutually exclusive oncogenic mutations in RET and RAS. J. Clin. Endocrinol. Metab. *98*, E364–E369.

Alzahrani, A.S., Alsaadi, R., Murugan, A.K., and Sadiq, B.B. (2016). TERT promoter mutations in thyroid cancer. Horm. Cancer *7*, 165–177.

Berger, M.F., and Mardis, E.R. (2018). The emerging clinical relevance of genomics in cancer medicine. Nat. Rev. Clin. Oncol. *15*, 353–365.

Boichard, A., Croux, L., Al Ghuzlan, A., Broutin, S., Dupuy, C., Leboulleux, S., Schlumberger, M., Bidart, J.M., and Lacroix, L. (2012). Somatic RAS mutations occur in a large proportion of sporadic RET-negative medullary thyroid carcinomas and extend to a previously unidentified exon. J. Clin. Endocrinol. Metab. *97*, E2031–E2035.

Camidge, D.R., Pao, W., and Sequist, L.V. (2014). Acquired resistance to TKIs in solid tumours: learning from lung cancer. Nat. Rev. Clin. Oncol. *11*, 473–481.

Cancer Genome Atlas Research Network (2014). Integrated genomic characterization of papillary thyroid carcinoma. Cell *159*, 676–690.

Cerrato, A., De Falco, V., and Santoro, M. (2009). Molecular genetics of medullary thyroid carcinoma: the quest for novel therapeutic targets. J. Mol. Endocrinol. *43*, 143–155.

Chang, Y.-S., Chang, C.-C., Huang, H.-Y., Lin, C.-Y., Yeh, K.-T., and Chang, J.-G. (2018). Detection of molecular alterations in Taiwanese patients with medullary thyroid cancer using whole-exome sequencing. Endocr. Pathol. *29*, 324–331.

Chen, Y., and Fu, L. (2011). Mechanisms of acquired resistance to tyrosine kinase inhibitors. Acta Pharm. Sin. B *1*, 197–207.

Ciampi, R., Mian, C., Fugazzola, L., Cosci, B., Romei, C., Barollo, S., Cirello, V., Bottici, V., Marconcini, G., Rosa, P.M., et al. (2013). Evidence of a low prevalence of RAS mutations in a large medullary thyroid cancer series. Thyroid *23*, 50–57.

Ciampi, R., Romei, C., Cosci, B., Vivaldi, A., Bottici, V., Renzini, G., Ugolini, C., Tacito, A., Basolo, F., Pinchera, A., and Elisei, R. (2012). Chromosome 10 and RET gene copy number alterations in hereditary and sporadic Medullary Thyroid Carcinoma. Mol. Cell. Endocrinol. *348*, 176–182.

Comoglio, P.M., Trusolino, L., and Boccaccio, C. (2018). Known and novel roles of the MET oncogene in cancer: a coherent approach to targeted therapy. Nat. Rev. Cancer *18*, 341–358.

Drosten, M., and Putzer, B.M. (2006). Mechanisms of Disease: cancer targeting and the impact of oncogenic RET for medullary thyroid carcinoma therapy. Nat. Clin. Pr. Oncol. *3*, 564–574.

Elisei, R., Cosci, B., Romei, C., Bottici, V., Renzini, G., Molinaro, E., Agate, L., Vivaldi, A., Faviana, P., Basolo, F., et al. (2008). Prognostic significance of somatic RET oncogene mutations in sporadic medullary thyroid cancer: a 10-year follow-up study. J. Clin. Endocrinol. Metab. *93*, 682–687.

Elisei, R., Molinaro, E., Agate, L., Bottici, V., Viola, D., Biagini, A., Matrone, A., Tacito, A., Ciampi, R., Vivaldi, A., and Romei, C. (2014). Ret oncogene and thyroid carcinoma. J. Genet. Syndr. Gene Ther. *5*, 10.

Elisei, R., Schlumberger, M.J., Müller, S.P., Schöffski, P., Brose, M.S., Shah, M.H., Licitra, L., Jarzab, B., Medvedev, V., Kreissl, M.C., et al. (2013). Cabozantinib in progressive medullary thyroid cancer. J. Clin. Oncol. *31*, 3639–3646.

Eng, C., Smith, D.P., Mulligan, L.M., Nagai, M.A., Healey, C.S., Ponder, M.A., Gardner, E., Scheumann, G.F., Jackson, C.E., Tunnacliffe, A.,

et al. (1994). Point mutation within the tyrosine kinase domain of the RET proto-oncogene in multiple endocrine neoplasia type 2B and related sporadic tumours. Hum. Mol. Genet. *3*, 237–241.

Guerra, A., Fugazzola, L., Marotta, V., Cirillo, M., Rossi, S., Cirello, V., Forno, I., Moccia, T., Budillon, A., and Vitale, M. (2012). A high percentage of BRAFV600E alleles in papillary thyroid carcinoma predicts a poorer outcome. J. Clin. Endocrinol. Metab. *97*, 2333–2340.

Heilmann, A.M., Subbiah, V., Wang, K., Sun, J.X., Elvin, J.A., Chmielecki, J., Sherman, S.I., Murthy, R., Busaidy, N.L., Subbiah, I., et al. (2016). Comprehensive genomic profiling of clinically advanced medullary thyroid carcinoma. Oncology *90*, 339–346.

Höppner, W., Dralle, H., and Brabant, G. (1998). Duplication of 9 base pairs in the critical cysteine rich domain of the ret proto-oncogene causes multiple endocrine neoplasia type 2A. Hum. Mutat. (*Suppl 1*), S128–S130. https://doi.org/10.1002/humu.1380110143.

Ji, J.H., Oh, Y.L., Hong, M., Yun, J.W., Lee, H.-W., Kim, D., Ji, Y., Kim, D.-H., Park, W.-Y., Shin, H.-T., et al. (2015). Identification of driving ALK fusion genes and genomic landscape of medullary thyroid cancer. PLoS Genet. *11*, e1005467.

Kamps, R., Brandão, R.D., van den Bosch, B.J., Paulussen, A.D.C., Xanthoulea, S., Blok, M.J., and Romano, A. (2017). Next-generation sequencing in oncology: genetic diagnosis, risk prediction and cancer classification. Int. J. Mol. Sci. *18*. https://doi.org/10.3390/ijms18020308.

Kouvaraki, M.A., Shapiro, S.E., Perrier, N.D., Cote, G.J., Gagel, R.F., Hoff, A.O., Sherman, S.I., Lee, J.E., and Evans, D.B. (2005). RET proto-oncogene: a review and update of genotype-phenotype correlations in hereditary medullary thyroid cancer and associated endocrine tumors. Thyroid *15*, 531–544.

Li, M.M., Datto, M., Duncavage, E.J., Kulkarni, S., Lindeman, N.I., Roy, S., Tsimberidou, A.M., Vnencak-Jones, C.L., Wolff, D.J., Younes, A., and Nikiforova, M.N. (2017). Standards and guidelines for the interpretation and reporting of sequence variants in cancer. J. Mol. Diagn. *19*, 4–23.

Moura, M.M., Cavaco, B.M., and Leite, V. (2015). RAS proto-oncogene in medullary thyroid carcinoma. Endocr. Relat. Cancer *22*, R235–R252.

Moura, M.M., Cavaco, B.M., Pinto, A.E., and Leite, V. (2011). High prevalence of RAS mutations in RET-negative sporadic medullary thyroid carcinomas. J. Clin. Endocrinol. Metab. *96*, E863–E868.

Neklason, D.W., Done, M.W., Sargent, N.R., Schwartz, A.G., Anton-Culver, H., Griffin, C.A., Ahnen, D.J., Schildkraut, J.M., Tomlinson, G.E., Strong, L.C., et al. (2011). Activating mutation in MET oncogene in familial colorectal cancer. BMC Cancer *11*, 424.

Nikiforov, Y.E., Carty, S.E., Chiosea, S.I., Coyne, C., Duvvuri, U., Ferris, R.L., Gooding, W.E., Hodak, S.P., LeBeau, S.O., Ohori, N.P., et al. (2014). Highly accurate diagnosis of cancer in thyroid nodules with follicular neoplasm/suspicious for a follicular neoplasm cytology by thyroseq V2 next-generation sequencing assay. Cancer *120*, 3627–3634.

Nikiforova, M.N., Wald, A.I., Roy, S., Durso, M.B., and Nikiforov, Y.E. (2013). Targeted next-generation sequencing panel (ThyroSeq) for detection of mutations in thyroid cancer. J. Clin. Endocrinol. Metab. *98*, 1852–1860.

Persani, L., de Filippis, T., Colombo, C., and Gentilini, D. (2018). GENETICS IN ENDOCRINOLOGY: genetic diagnosis of endocrine diseases by NGS: novel scenarios and unpredictable results and risks. Eur. J. Endocrinol. *179*, R111–R123.

Romei, C., Ciampi, R., and Elisei, R. (2016). A comprehensive overview of the role of the RET proto-oncogene in thyroid carcinoma. Nat. Rev. Endocrinol. *12*, 192–202.

Romei, C., Cosci, B., Renzini, G., Bottici, V., Molinaro, E., Agate, L., Passannanti, P., Viola, D., Biagini, A., Basolo, F., et al. (2011). RET genetic screening of sporadic medullary thyroid cancer (MTC) allows the preclinical diagnosis of unsuspected gene carriers and the identification of a relevant percentage of hidden familial MTC (FMTC). Clin. Endocrinol. *74*, 241–247.

Romei, C., Ugolini, C., Cosci, B., Torregrossa, L., Vivaldi, A., Ciampi, R., Tacito, A., Basolo, F., Materazzi, G., Miccoli, P., et al. (2012). Low prevalence of the somatic M918T RET mutation in micro-medullary thyroid cancer. Thyroid *22*, 476–481.

Ruark, E., Snape, K., Humburg, P., Loveday, C., Bajrami, I., Brough, R., Rodrigues, D.N., Renwick, A., Seal, S., Ramsay, E., et al. (2013). Mosaic PPM1D mutations are associated with predisposition to breast and ovarian cancer. Nature *493*, 406–410.

Simbolo, M., Mian, C., Barollo, S., Fassan, M., Mafficini, A., Neves, D., Scardoni, M., Pennelli, G., Rugge, M., Pelizzo, M.R., et al. (2014). High-throughput mutation profiling improves diagnostic stratification of sporadic medullary thyroid carcinomas. Virchows Arch. *465*, 73–78.

Vigna, E., Gramaglia, D., Longati, P., Bardelli, A., and Comoglio, P.M. (1999). Loss of the exon encoding the juxtamembrane domain is essential for the oncogenic activation of TPR-MET. Oncogene *18*, 4275–4281.

Viola, D., Valerio, L., Molinaro, E., Agate, L., Bottici, V., Biagini, A., Lorusso, L., Cappagli, V., Pieruzzi, L., Giani, C., et al. (2016). Treatment of advanced thyroid cancer with targeted therapies: ten years of experience. Endocr. Relat. Cancer *23*, R185–R205.

Vuong, H.G., Odate, T., Ngo, H.T.T., Pham, T.Q., Tran, T.T.K., Mochizuki, K., Nakazawa, T., Katoh, R., and Kondo, T. (2018). Clinical significance of RET and RAS mutations in sporadic medullary thyroid carcinoma: a meta-analysis. Endocr. Relat. Cancer *25*, 633–641. https://doi.org/10.1530/ERC-18-0056.

Wang, Q., Mehmood, A., Wang, H., Xu, Q., Xiong, Y., and Wei, D.Q. (2019). Computational screening and analysis of lung cancer related non-synonymous single nucleotide polymorphisms on the human kirsten rat sarcoma gene. Molecules *24*. https://doi.org/10.3390/molecules24101951.

Wasenius, V.M., Hemmer, S., Karjalainen-Lindsberg, M.L., Nupponen, N.N., Franssila, K., and Joensuu, H. (2005). MET receptor tyrosine kinase sequence alterations in differentiated thyroid carcinoma. Am. J. Surg. Pathol. *29*, 544–549.

Wei, S., LiVolsi, V.A., Montone, K.T., Morrissette, J.J.D., and Baloch, Z.W. (2016). Detection of molecular alterations in medullary thyroid carcinoma using next-generation sequencing: an institutional experience. Endocr. Pathol. *27*, 359–362.

Wells, S.A., Jr., Gosnell, J.E., Gagel, R.F., Moley, J., Pfister, D., Sosa, J.A., Skinner, M., Krebs, A., Vasselli, J., and Schlumberger, M. (2010). Vandetanib for the treatment of patients with locally advanced or metastatic hereditary medullary thyroid cancer. J. Clin. Oncol. *28*, 767–772.

ISCI, Volume *20*

Supplemental Information

Genetic Landscape of Somatic Mutations in a Large Cohort of Sporadic Medullary Thyroid Carcinomas Studied by Next-Generation Targeted Sequencing

Raffaele Ciampi, Cristina Romei, Teresa Ramone, Alessandro Prete, Alessia Tacito, Virginia Cappagli, Valeria Bottici, David Viola, Liborio Torregrossa, Clara Ugolini, Fulvio Basolo, and Rossella Elisei

SUPPLEMENTAL INFORMATION

No	No in the report	Genetic Variation	VAF (%)
1	6	RET c.2753T>C; p.M918T (s)	43,7
2	11	RET c.2753T>C; p.M918T (s)	40,1
3	14	RET c.2753T>C; p.M918T (s)	32.03
4	15	RET c.2753T>C; p.M918T (s)	11,8
5	22	RET c.2753T>C; p.M918T (s)	42,5
6	23	RET c.2753T>C; p.M918T (s)	50,8
7	43	RET c.2753T>C; p.M918T (s)	92,7
8	50	RET c.2753T>C; p.M918T (s)	44,7
9	51	RET c.2753T>C; p.M918T (s)	28,9
10	53	RET c.2753T>C; p.M918T (s)	38,6
11	62	RET c.2753T>C; p.M918T (s)	62,2
12	63	RET c.2753T>C; p.M918T (s)	41,0
13	85	RET c.2753T>C; p.M918T (s)	44,0
14	89	RET c.2753T>C; p.M918T (s)	45,8
15	90	RET c.2753T>C; p.M918T (s)	55,5
16	92	RET c.2753T>C; p.M918T (s)	27,4
17	93	RET c.2753T>C; p.M918T (s)	48,1
18	94	RET c.2753T>C; p.M918T (s)	59,0
19	96	RET c.2753T>C; p.M918T (s)	35,7
20	101	RET c.2753T>C; p.M918T (s)	44,8
21	105	RET c.2753T>C; p.M918T (s)	20,3
22	110	RET c.2753T>C; p.M918T (s)	42,3
23	118	RET c.2753T>C; p.M918T (s)	17,0
24	121	RET c.2753T>C; p.M918T (s)	34,6
25	123	RET c.2753T>C; p.M918T (s)	39,0
26	125	RET c.2753T>C; p.M918T (s)	37,4
27	127	RET c.2753T>C; p.M918T (s)	18,0
28	131	RET c.2753T>C; p.M918T (s)	46,6
29	134	RET c.2753T>C; p.M918T (s)	41,0
30	135	RET c.2753T>C; p.M918T (s)	28,9
31	136	RET c.2753T>C; p.M918T (s)	38,3
32	139	RET c.2753T>C; p.M918T (s)	41,5
33	142	RET c.2753T>C; p.M918T (s)	37,0
34	170	RET c.2753T>C; p.M918T (s)	36,6
35	185	RET c.2753T>C; p.M918T (s)	46,5
36	191	RET c.2753T>C; p.M918T (s)	42,4
37	199	RET c.2753T>C; p.M918T (s)	29,6
38	203	RET c.2753T>C; p.M918T (s)	39,7
39	204	RET c.2753T>C; p.M918T (s)	64,6
40	205	RET c.2753T>C; p.M918T (s)	22,6
41	211	RET c.2753T>C; p.M918T (s)	33,0
42	238	RET c.2753T>C; p.M918T (s)	40,6
43	247	RET c.2753T>C; p.M918T (s)	43,1
44	248	RET c.2753T>C; p.M918T (s)	46,3
45	249	RET c.2753T>C; p.M918T (s)	19,3
46	257	RET c.2753T>C; p.M918T (s)	4,4
47	258	RET c.2753T>C; p.M918T (s)	19,0
48	262	RET c.2753T>C; p.M918T (s)	38,1
49	303	RET c.2753T>C; p.M918T (s)	39,6
50	305	RET c.2753T>C; p.M918T (s)	27,7
51	313	RET c.2753T>C; p.M918T (s)	29,7
52	314	RET c.2753T>C; p.M918T (s)	44,7
53	316	RET c.2753T>C; p.M918T (s)	31,5
54	317	RET c.2753T>C; p.M918T (s)	32,4
55	88	RET c.2753T>C; p.M918T (s)	19,7
		KRAS c.389C>T; p.A130V (g)	44,9
56	41	RET c.2753T>C; p.M918T (s)	47,3
		RET c.2774A>C; p.D925A (s)	46,7
57	242	RET c.2753T>C; p.M918T (s)	32,2

		RET c.890G>A; p.R297H (s)	11,8
58	196	RET c.2753T>C; p.M918T (s)	12,3
		RET c.2497C>T; p.R833C (s)	25
		RET c.2671T>G; p.S891A (s)	20,35
		MET c.3029C>T; p.T1010I (nv)	18,6
59	39	RET c.2753T>C; p.M918T (s)	3,0
		HRAS c.182A>G; p.Q61R (s)	34,4
60	140	RET c.2753T>C; p.M918T (s)	39,0
		KRAS c.544A>G; p.K182E (nv)	20
61	178	RET c.1900T>C; p.C634R (s)	38,4
62	184	RET c.1900T>C; p.C634R (s)	36,0
63	208	RET c.1900T>C; p.C634R (s)	20,6
64	241	RET c.1900T>C; p.C634R (s)	15,8
65	261	RET c.1900T>C; p.C634R (s)	43,3
66	263	RET c.1900T>C; p.C634R (s)	28,3
67	310	RET c.1900T>C; p.C634R (s)	35,3
68	83	RET c.1902C>G; p.C634W (s)	24,6
69	111	RET c.1902C>G; p.C634W (s)	33,0
70	126	RET c.1902C>G; p.C634W (s)	60,7
71	177	RET c.1902C>G; p.C634W (s)	24,5
72	188	RET c.1902C>G; p.C634W (s)	26,9
73	176	RET c.1902C>G; p.C634W (s)	17,3
		NRAS c.53C>T; p.A18V (s)	7,5
74	253	RET c.1902C>G; p.C634W (s)	11,6
		MET c.3029C>T; p.T1010I (s)	50,1
75	12	RET c.1901G>A; p.C634Y (s)	43,2
76	91	RET c.1901G>A; p.C634Y (s)	37,3
		RET c.644G>T; p.R215L (g)	49,9
77	124	RET c.1901G>T; p.C634F (s)	39,0
78	304	RET c.1900T>A; p.C634S (s)	28,7
79	54	RET c.2694_2705delTGTTTATGAAGA; p.D898_E901del (s)	27,9
80	141	RET c.2694_2705delTGTTTATGAAGA; p.D898_E901del (s)	54,1
81	215	RET c.2694_2705delTGTTTATGAAGA; p.D898_E901del (s)	38,7
82	201	RET c.2694_2705delTGTTTATGAAGA; p.D898_E901del (s)	26,6
		PPM1D c.1405A>G; p.K469E (g)	37,5
83	132	RET c.2694_2705delTGTTTATGAAGA; p.D898_E901del (s)	30,9
		RET c.2710T>C; p.S904P (s)	30,8
84	128	RET c.1908_1909insTGCCGCACG; p.T636_V637delinsCRT (s)	35,4
85	61	RET c.1899_1900delGTinsTG; p.C634G/L633L (s)	43,2
86	186	RET c.1894_1899delGAGCTG; p.E632_L633del (s)	95,2
87	302	RET c.1894_1902delGAGCTGTGC; p.E632_C634del (s)	42,9
89	66	RET c.1894_1904delGAGCTGTGCCG; c.1912_1918delATCGCAG; c.1908G>T; p. E632_A639delinsHR (s)	48,0
88	122	RET c.1886_1891delTGTGCG; p.L629_D631delinsH (s)	38,4
90	119	RET c.2647_2648delGCinsTT; p.A883F (s)	13,8
91	97	RET c.2647_2648delGCinsTT; p.A883F (s)	31,1
92	309	RET c.2647_2648delGCinsTT; p.A883F (s)	14,9
93	27	RET c.1858T>C; p.C620R (s)	14,4
94	100	RET c.1858T>C; p.C620R (s)	55,5
95	169	RET c.1858T>C; p.C620R (s)	41,5
		MET c.3029C>T; p.T1010I (nv)	6,7
96	75	RET c.2671T>G; S891A (s)	47,0
97	82	RET c.2671T>G; S891A (s)	20,8
98	137	RET c.1852T>C; C618R (s)	31,4
99	3	RET c.1852T>G; C618G (nv)	40,5
		TP53 c.847C>T; p.R283C (nv)	48,1
101	175	RET c.1888T>C; C630R (s)	45,1
100	252	RET c.3071C>T; p.S1024F (s)	17,6
102	7	HRAS c.182A>G; p.Q61R (s)	50.7
103	10	HRAS c.182A>G; p.Q61R (s)	28,0
104	17	HRAS c.182A>G; p.Q61R (s)	41,8
105	26	HRAS c.182A>G; p.Q61R (s)	39,8
106	44	HRAS c.182A>G; p.Q61R (s)	26,2
107	47	HRAS c.182A>G; p.Q61R (s)	38,2
108	57	HRAS c.182A>G; p.Q61R (s)	19,0

109	67	HRAS c.182A>G; p.Q61R (s)	41,3
110	73	HRAS c.182A>G; p.Q61R (s)	39,7
111	87	HRAS c.182A>G; p.Q61R (s)	46,0
112	95	HRAS c.182A>G; p.Q61R (s)	41,1
113	112	HRAS c.182A>G; p.Q61R (s)	29,6
114	182	HRAS c.182A>G; p.Q61R (s)	22,0
115	189	HRAS c.182A>G; p.Q61R (s)	16,4
116	207	HRAS c.182A>G; p.Q61R (s)	36,6
117	210	HRAS c.182A>G; p.Q61R (s)	43,8
118	250	HRAS c.182A>G; p.Q61R (s)	7,5
119	315	HRAS c.182A>G; p.Q61R (s)	59,6
120	20	HRAS c.182A>G; p.Q61R (s)	41,7
		MET c.3029C>T; p.T1010I (g)	51,4
121	60	HRAS c.181C>A; p.Q61K (s)	37,4
122	70	HRAS c.181C>A; p.Q61K (s)	25,3
123	99	HRAS c.181C>A; p.Q61K (s)	47,9
124	133	HRAS c.181C>A; p.Q61K (s)	38,7
125	246	HRAS c.181C>A; p.Q61K (s)	31,5
126	307	HRAS c.181C>A; p.Q61K (s)	31,4
127	74	HRAS c.182A>T; p.Q61L (s)	44,9
128	19	HRAS c.37G>C; p.G13R (s)	42,5
129	56	HRAS c.37G>C; p.G13R (s)	36,1
130	65	HRAS c.37G>C; p.G13R (s)	41,4
131	214	HRAS c.37G>C; p.G13R (s)	35,2
132	251	HRAS c.37G>C; p.G13R (s)	23,2
		MET c.3029C>T; p.T1010I (s)	8,3
133	5	KRAS c.34G>C; p.G12R (s)	40,0
134	69	KRAS c.34G>C; p.G12R (s)	42,7
135	71	KRAS c.34G>C; p.G12R (s)	29,0
136	172	KRAS c.34G>C; p.G12R (s)	42,8
137	179	KRAS c.34G>C; p.G12R (s)	42,5
138	190	KRAS c.34G>C; p.G12R (s)	44,2
139	197	KRAS c.34G>C; p.G12R (s)	30,2
140	212	KRAS c.34G>C; p.G12R (s)	24,0
141	244	KRAS c.34G>C; p.G12R (s)	45,2
142	21	KRAS c.182A>G; Q61R (s)	50,3
143	239	KRAS c.183A>T; Q61H (s)	10,5
144	174	KRAS c.437C>T; p.A146V (s)	36,0
145	8	NRAS c.181C>A; p.Q61K (s)	20,6
146	52	TSHR c.1888A>C; p.I630L (s)	31,0
		TP53 c.472C>T; p.R158C (g)	52,8
147	195	EIF1AX c.404G>C; G135A (*)	41,4
148	198	CHK2 c.341G>A; W114* (nv)	10,1

Table S1: Related to Figure 1. List of genetic variations found in 148 sMTC

(**s**) verified somatic; n.v. no detectable by direct sequencing; (*****) validated as somatic in tissue but blood not available for germline validation

TRANSPARENT METHODS

Patient cohort

We studied surgically removed tumoral tissues from 209 sMTC cases: 175/209 (83.7%) were primary tumors, 33/209 (15.8%) were lymph-node metastases and 1/209 (0.5%) showed tumor recurrence. All patients were diagnosed and followed at the Unit of Endocrinology of the Department of Clinical and Experimental Medicine of the University of Pisa. The diagnosis of sMTC was based on the absence of germline *RET* mutations, absence of a familial history of the disease, and negative clinical and laboratory data for the presence of other endocrine neoplasia. Informed consent forms for *RET* genetic screening and other clinical procedures were signed by each of the investigated subjects, and the present study was approved by the Institutional Review Board.

The clinical and pathological data of the patients were collected in a database and were available for correlation with the molecular data. Of 209 sMTC patients, 86 were male and 123 female with a mean age at the diagnosis of 54.4 yrs. [median: 56; range 20-87 yrs.]. According to the AJCC Cancer Staging System, 7th Edition (Edge and Compton, 2010), 63/209 (30.1%) were at stage I, 13/209 (6.2%) at stage II, 30/209 (14.4%) at stage III and 74/209 (35.4%) at stage IV; for 29/209 (13.9%), the data were not available. The mean tumor size was 2.07cm [median: 1.6; range: 0.1-9.5 cm] calculated on 157/209 (75.1%) patients.

According to their clinical status, defined based on both the serum calcitonin levels and imaging results (i.e., neck ultrasound, computed tomography scan and bone scintigraphy), patients were classified into three groups: A) “disease free” patients [n= 85/209 (40.7%)]; B) patients with “persistent disease” only at the biochemical level [n= 24/209 (11.5%)]; C) patients with evidence of metastatic disease and/or dead patients [n=69/209 (33.0%)]. The data on outcome were not available in 31/209 (14.8%) cases. At the time of the present study, the mean follow-up was 84.93 months [median: 65; range 3–324 months].

RET gene somatic mutation analysis by Sanger direct sequencing in exons 10, 11, 13, 14, 15 and

16 and exons 2, 3, 4 of was previously performed on 148 sMTC; moreover, in 65 of these cases we sequenced exons 2, 3, 4 of *HRAS*, *KRAS* and *NRAS* mutations following standard screening procedures in our laboratory (Ciampi et al., 2013; Romei et al., 2011).

Tissue samples were collected at surgery and snap-frozen at -80° when patients were operated in Pisa; for the others, formalin-fixed paraffin-embedded (FFPE) tissues were used. Blood samples were collected in EDTA and were available for most of the cases studied.

Nucleic acid isolation from tumoral tissues

Snap-frozen tumoral tissue was available in 159 cases, while FFPE tissue was available for the other 50 cases.

For most cases, genomic DNA was extracted using the automated method Maxwell16® (Promega, Madison, WI, USA) using the following kits: Maxwell® 16 FFPE Plus LEV Blood DNA Purification kit for frozen tissues and Maxwell® 16 FFPE Plus LEV DNA Purification kit for FFPE tissues. Approximately 40mg of internal tumoral tissue was used in frozen samples, while the tumoral areas with more than 50% of tumoral cells were collected from four 4-µm unstained slides; DNA was finally eluted in 300 µl of DNase and RNase-free water for blood DNA and 50 µl for tissue DNA and quantified using the Qubit 3 fluorometer (Invitrogen, Calsbad, CA, USA) and the Qubit™ dsDNA HS Assay kit.

Ion S5 targeted sequencing

NGS libraries were obtained using a thyroid-specific custom panel designed using the AmpliSeq Designer tool available from Thermo Fisher (https://www.ampliseq.com/). The DNA panel contained 212 couples of primers that can amplify 20.34 kb of the genome including the following regions: *RET* (entire CDS + 5'- and 3'-UTR), *HRAS* (entire CDS), *KRAS* (entire CDS), *NRAS*

(entire CDS), *TP53* (exons 5-9), *GNAS* (exons 8-9), *EIFA1X* (exons 1, 2, 5, 6), *AKT1* (exon 3), *MET* (exon 14), *CHEK2* (exons 4, 5, 7, 12, 14), *BRAF* (exon 15), *CTNNB1* (exon 3), *STK11* (exons 1, 7, 8), *PTEN* (exons 5-8), *PIK3CA* (exons 9, 20), *PPM1D* (exons 5, 6), and*TSHR* (exon 10).

Twenty-five nanograms of tumoral genomic DNA were amplified with specific primers for the above-described panel using the Ion AmpliSeq library kit 2.0 (Life Technologies, Calsbad, CA, USA)following manufacturer's instructions; different samples were barcoded using the Ion Xpress Barcode Adapters kit (Life Technologies, Calsbad, CA, USA). DNA library quantification was performed using the Qubit™ dsDNA HS Assay (Life Technologies), and 100pM dilutions were pooled together. The number of samples pooled together was calculated according to the desired vertical coverage of reads (2000X). Emulsion clonal PCR was performed using the OneTouch (OT2) System (Life Technologies), and enrichment of Ion Sphere Particles (ISP) was performed using the Enrichment System (ES) (Life Technologies, Calsbad, CA, USA). Finally, massively parallel sequencing was performed on a 520 Chip in an Ion S5 deep sequencer (Ion Torrent; Applied Biosystem, Calsbad, CA, USA) following the manufacturer's instructions.

NGS Data analysis

Raw sequencing data analysis was analyzed using Torrent Suite Software v.5.6 (Life Technologies) and included alignment to the hg19 human reference genome, quality score assignment, variant calling and coverage analysis. The data were further analyzed by Ion Reporter v.5.6 (https://ionreporter.thermofisher.com) with a bioinformatics workflow that calculated the Phred Quality score and performed annotation to dbSNP, COSMIC, and ExAC databases; data were finally filtered to several *in silico* prediction tools of pathogenicity (PhyloP, SIFT, Grantham, PolyPhen and FATHMM).

The system could evaluate the variant allele frequency (VAF) of the mutated allele within the sample. The VAF value for the heterozygous germline variations was 50% while, for somatic variations, it was variable depending on the abundance of the tumor cells with respect to normal

cells in the analyzed sample, as well as on the heterogeneity of mutations in tumoral cells (Li et al., 2017). We arbitrarily set the clinical sensitivity of VAF $\geq$ 10% for variations already known to be drivers (i.e., *RET, HRAS, KRAS*); clinical sensitivity was lowered to VAF $\geq$ 5% for putative additional mutations as previously suggested (Nikiforov et al., 2014). Nevertheless, driver alterations in typical hotspots (such as *RET* M918T mutation) with a lower VAF value were considered positive if validated by Sanger direct sequencing.

With a few exceptions, all variants detected were validated in the same tissue DNA by direct sequencing using specific conditions and primers, while novel and unconventional variations were tested on blood genomic DNA to assess their somatic or germline origin.

TERT promoter mutation analysis

Direct sequencing analysis of the *TERT* gene promoter hotspot mutations C228T and C250T was performed on all cases studied. Amplification of DNA obtained from frozen samples was performed using F: 5'-CTGGCGTCCCTGCACCCTGG-3' and R: 5'-ACGAACGTGGCCAGCGGCAG-3' as previously described (Romei et al., 2018), while oligos for FFPE sample analysis were newly designed: F: 5'-CCCTTCACCTTCCAGCTCC-3', R: 5'-CAGCGCTGCCTGAAACTC-3'. Sanger direct sequencing analysis was performed using the AbiPrism 3130xl Genetic Analyzer (Applied Biosystems, Calsbad, CA, USA).

Whole exome sequencing

Six sMTC, 4 negative at the targeted sequencing analysis for any mutation and 2 positive only for *RET* somatic mutation were further analyzed by whole exome sequencing (WES) through an external service (IGA Technology Services Srl, Udine, Italy) to look for any other possible gene alteration not detected with our gene mutation panel.

Statistical analysis

Statistical analysis and graphs were generated using Prism GraphPad (version 8) (https://www.graphpad.com/). The different prevalence values of categorical data within the different mutational status were analyzed by Chi-squared test. The differences in the outcome and mutational status categories were evaluated by 1-way ANOVA and unpaired Student's t-test with Welch's correction in the case of significant differences between variances. The correlation between the VAF and tumor size was evaluated by a linear regression curve, while differences in survival between *RET*- and *RAS*-mutated sMTC cases were analyzed by Kaplan-Meier curves with the log-rank test. Differences were considered statistically significant when the *P* value was less than 0.05.

SUPPLEMENTAL REFERENCES

Ciampi, R., Mian, C., Fugazzola, L., Cosci, B., Romei, C., Barollo, S., Cirello, V., Bottici, V., Marconcini, G., Rosa, P.M., Borrello, M.G., Basolo, F., Ugolini, C., Materazzi, G., Pinchera, A., Elisei, R., 2013. Evidence of a low prevalence of RAS mutations in a large medullary thyroid cancer series. Thyroid 23, 50–7.

Edge, S.B., Compton, C.C., 2010. The american joint committee on cancer: The 7th edition of the AJCC cancer staging manual and the future of TNM. Ann. Surg. Oncol. https://doi.org/10.1245/s10434-010-0985-4

Li, M.M., Datto, M., Duncavage, E.J., Kulkarni, S., Lindeman, N.I., Roy, S., Tsimberidou, A.M., Vnencak-Jones, C.L., Wolff, D.J., Younes, A., Nikiforova, M.N., 2017. Standards and Guidelines for the Interpretation and Reporting of Sequence Variants in Cancer. J. Mol. Diagnostics. https://doi.org/10.1016/j.jmoldx.2016.10.002

Nikiforov, Y.E., Carty, S.E., Chiosea, S.I., Coyne, C., Duvvuri, U., Ferris, R.L., Gooding, W.E., Hodak, S.P., LeBeau, S.O., Ohori, N.P., Seethala, R.R., Tublin, M.E., Yip, L., Nikiforova, M.N., 2014. Highly accurate diagnosis of cancer in thyroid nodules with follicular neoplasm/suspicious for a follicular neoplasm cytology by thyroseq V2 next-generation sequencing assay. Cancer. https://doi.org/10.1002/cncr.29038

Romei, C., Cosci, B., Renzini, G., Bottici, V., Molinaro, E., Agate, L., Passannanti, P., Viola, D., Biagini, A., Basolo, F., Ugolini, C., Materazzi, G., Pinchera, A., Vitti, P., Elisei, R., 2011. RET genetic screening of sporadic medullary thyroid cancer (MTC) allows the preclinical diagnosis of unsuspected gene carriers and the identification of a relevant percentage of hidden familial MTC (FMTC). Clin Endocrinol 74, 241–247.

Romei, C., Tacito, A., Molinaro, E., Piaggi, P., Cappagli, V., Pieruzzi, L., Matrone, A., Viola, D., Agate, L., Torregrossa, L., Ugolini, C., Basolo, F., De Napoli, L., Curcio, M., Ciampi, R., Materazzi, G., Vitti, P., Elisei, R., 2018. Clinical, pathological and genetic features of anaplastic and poorly differentiated thyroid cancer: A single institute experience. Oncol. Lett. https://doi.org/10.3892/ol.2018.8470